Chapter 3

The Role of Selection in Shaping the Craniomandibular Morphology of *Paranthropus*

Nomawethu Hlazo, Department of Archaeology, University of Cape Town, South Africa; *Human Evolution Research Institute, University of Cape Town, South Africa, nomawethu.hlazo90@gmail.com

Lauren Schroeder, Department of Anthropology, University of Toronto Mississauga, Canada; Human Evolution Research Institute, University of Cape Town, South Africa

Terrence Ritzman, Human Evolution Research Institute, University of Cape Town, South Africa; Department of Anatomy, Midwestern University, Downers Grove, IL, USA

Rebecca R. Ackermann, Department of Archaeology, University of Cape Town, South Africa; Human Evolution Research Institute, University of Cape Town, South Africa.

Abstract

Craniodental robusticity in *Paranthropus* has been interpreted as evidence that species in this genus share an adaptation to a diet of hard foods. However, recent research on craniodental morphology, microwear, biomechanics, and stable isotopes has suggested that substantial variation exists within *Paranthropus*, both in terms of the ecological niches occupied by the species and the inferred amount of consumed hard and compliant foods. Rather than pointing to a common adaptive suite, these studies suggested that the species were adaptively distinct from each other. However, current approaches to understanding cranio-mandibular morphology do not present a clear picture of how these species-specific adaptations differ. It is also unclear whether all aspects of morphology that have been attributed to adaptation are indeed adaptive, rather than the products of non-adaptive processes. This study examines

variation in fossil specimens assigned to the three *Paranthropus* species (*n*=39) using an approach that tests for adaptive divergence in morphology against a null hypothesis of random change (i.e., drift). Extant species (*Homo sapiens*, *Gorilla gorilla*, *Pan troglodytes*; *n*=293) act as analogues for within species variance/covariance (V/CV) in the fossil taxa. Results reveal a high magnitude of variation within and between species across mandibular/cranial regions, especially when *Paranthropus robustus* individuals from Drimolen are included. Neutrality tests detect adaptive divergence between *P. robustus* and *Paranthropus boisei* and *Australopithecus africanus*, but not between *Paranthropus aethiopicus* and *P. boisei*. Reconstructed selection vectors indicate that directional selection has driven size related changes in mandibular and tooth dimensions, as well as in the cranium, resulting in a range of morphological responses including considerable evidence for correlated selection. Additional studies are needed to further investigate the nature of adaptive and non-adaptive divergence in these fossil hominins.

Keywords: Variation, evolutionary process, genetic drift, adaptation

Running head: *Role of Selection in Morphology*

Introduction

Previous research on the genus *Paranthropus* has highlighted a suite of traits linked to overall cranio-mandibular robusticity shared among its three recognised species (*P. aethiopicus, P. boisei and P. robustus*). The megadont *Paranthropus* taxa are defined by molarized premolars, large molar tooth crowns, both with thick enamel, small anterior dentition (Kimbel 2006; Wood 2010), a robust mandibular corpus, combined with a flat, broad face with anteriorly- placed flaring zygomatic arches (Broom 1938b; Rak 1983; Leakey and Walker 1988; McCollum 1999). These features have collectively been considered adaptations to process a diet of hard and/or tough abrasive foods (Ungar et al. 2008; Rabenold and Pearson 2011; Williams 2015). Indeed, hypotheses surrounding the evolution of these shared traits, as well as the evolutionary scenarios used to explain the diversification of this genus, have traditionally been dominated by adaptive narratives (i.e., the traits result from natural selection driving morphological divergence).

Despite the traditional dominance of adaptive narratives, recent research on craniodental morphology, macrowear and microwear, stable isotopes, and biomechanics has shown that substantial variation exists within *Paranthropus*, both in terms of the ecological niches occupied by the species and the amount of hard foods consumed (Ungar et al. 2008; Lucas et al. 2013; Sponheimer et al. 2013; Martinez et al. 2016). These findings suggest that the three species were evolving similar morphology in response to different selective (or other evolutionary) pressures. In other words, this evidence implies that different, species-specific evolutionary scenarios (including both adaptive and non-adaptive processes) may explain the morphological differences seen among *Paranthropus* species in eastern and southern Africa, and species-specific evolutionary scenarios could also explain the differences between *P. boisei* and *P. aethiopicus*. Divergent and complex species-specific scenarios make sense in light of the wide geographical distribution and temporal range of the

genus (Fig. 3.1) (Cerling et al. 2011; Ungar and Sponheimer 2011; Sponheimer et al. 2013; Smith et al. 2015; Williams 2015). However, simpler traditional adaptive explanations still persist and, to date, little attention has been paid to understanding the potential role of non-adaptive processes in the diversification of this genus.

The dominance of adaptive narratives in explanations of hominin evolution and divergence has not been limited to *Paranthropus*. For many decades, the emergence and diversification of most of the hominin lineage has largely been framed as resulting from adaptation with little consideration of contributions from random events/effects. Ackermann and Cheverud (2002; 2004) proposed that some of the diversity in primate and hominin evolution may have been the product of neutral (random) evolution acting on morphological features (see also Weaver et al. 2007; Schroeder et al. 2014; Schroeder 2015). This observation was consistent with research showing that evolutionary divergence results from a combination of forces (genetic drift, mutation, gene flow and natural selection) working together to create change at a molecular and phenotypic level (e.g., Kimura 1968; Lande 1976; Kimura 1991; Arnold 1992).

Kimura (1968; 1991) outlined how random changes in allele frequency and/or random mutations occurring at different loci can elicit evolutionary change. This theory has encouraged researchers to use genetic drift as a null hypothesis, with natural selection as an alternative hypothesis. The hypothesis of genetic drift is statistically testable and allows for predictions (Lande 1977; Lande 1979) at both the molecular (Kimura 1991) and phenotypic levels (e.g., Lofsvold 1988; Roseman 2004; Ackermann and Cheverud 2004; Marriog and Cheverud 2004; Weaver et al. 2007; Schroeder et al. 2014; Schroeder and Ackermann 2017; Schroeder and von Cramon-Taubadel 2017). If the null hypothesis of drift is rejected, then adaptive non-random forces may have contributed to evolutionary change. However, if the null hypothesis is not rejected, it indicates that these neutral forces may have contributed to

evolutionary changes (Ackermann and Cheverud 2002; Ackermann and Cheverud 2004). It is important to note here that a rejection of drift does not provide direct evidence of selection, nor does a failure to reject drift prove that drift is the sole contributor to lineage diversification, as both of these evolutionary forces play significant roles in species divergence. Although, like many approaches, this method has limitations, it has been used successfully to investigate evolutionary changes in different hominin lineages (Roseman 2004; Ackermann and Cheverud 2004; Weaver et al. 2007; Schroeder et al. 2014; Schroeder and Ackermann 2017), not only to identify non-adaptive mechanisms of evolution, but also to provide a means to understand and characterize the action and effects of selection, when it is demonstrated to have played a role in diversification (e.g., Ackermann and Cheverud 2004; Schroeder and Ackermann 2017).

In this context, given the large amount of variability among *Paranthropus* taxa (Hlazo 2015; Hlazo 2018) and the emerging evidence for niche differentiation among *Paranthropus* species, the objectives of this study are: 1) to test whether the non-adaptive evolutionary process of genetic drift might play a role in structuring inter-specific diversity in *Paranthropus*, and, 2) to quantitatively characterize selection when drift is rejected, and demonstrate its role in regional diversification in *Paranthropus*.

PLACE FIGURE 3.1 ABOUT HERE; WIDTH = 1.5 COLUMNS

Materials

Data Collection

Our fossil hominin sample (Table 3.1) consisted of 39 *Paranthropus* specimens from all three recognized species and includes material from Swartkrans and Drimolen and specimens from

East and West Turkana and Olduvai Gorge. The majority of the specimens were adults. Subadults were also included in a small number of analyses to maximize sample size, and analyses that included subadults are indicated throughout. Three specimens of *Australopithecus africanus* were also included to provide context and assess the relationship between *Paranthropus* and *Australopithecus* within southern Africa. Relevant *Australopithecus afarensis* material was not available for this study. Large samples of extant *H. sapiens*, *P. troglodytes* and *G. gorilla* crania and mandibles were used to generate models of within species variability. All data were derived from 3D models created from surface scans from a previous study (Schroeder and Ackermann 2017) using a NextEngine Desktop Laser Scanner and CT scans from a previous study (Copes 2012; Copes and Kimbel 2016) converted to surface scans (.ply) using Avizo.

PLACE TABLE 3.1 ABOUT HERE; WIDTH = 1.5 COLUMNS

Landmark Protocol

Whenever possible, 56 homologous 3D landmarks (44 on the cranium and 12 on the mandible) were collected from specimens (Table 3.2; Fig. 3.2; Fig. 3.3). From these landmarks, a maximum of 74 inter-landmark distances were extracted (described in the footnote of Table 3.2).

Preservation dictated which landmarks and inter-landmark distances could be collected from each fossil specimen. Inter-landmark distances were calculated for both left and right sides (bilateral) and averaged. If only one side was preserved, unilateral inter-landmark distances were used, following Schroeder (2007; 2015). Bilateral inter-landmark

distances were collected for all comparative extant specimens and the mean of the two sides was calculated.

PLACE FIGURE 3.2 ABOUT HERE; WIDTH = 1.5 COLUMNS

PLACE FIGURE 3.3 ABOUT HERE; WIDTH = 1.5 COLUMNS

PLACE TABLE 3.2 ABOUT HERE; WIDTH = 1.5 COLUMNS

Methods

Many paleoanthropological studies are affected by: (1) distortion and damage to fossil specimens (due to mining, postmortem matrix expansion, and other taphonomic processes), and (2) small sample sizes. To mitigate these issues, a balance was struck between the number of variables and the size of the samples. Previous studies on hominin craniofacial remains (e.g., Ackermann 1998; Schroeder 2015) have struck this balance by either maximizing the number of individuals and having a smaller number of shared variables, or maximizing the number of variables with a reduced of number specimens. However, the latter can be problematic if the methods that are employed require large samples, as is the case for methods that require estimations of variance and covariance (Ackermann 2002; Ackermann 2009). In light of these issues, nine analyses were designed to best cover shared morphological regions, maximizing variable or specimen number, or both, whenever possible (see Table 3.3 for a description of each analysis). Comparative extant taxa were used as analogues/models to estimate within-taxon variation in the fossil sample. As this approach assumes that the fossil and extant groups have similar patterns of variation (Ackermann

2009), we used three extant taxa (*G. gorilla*, *P. troglodytes* and *H. sapiens*) to avoid relying on a single taxon as an analogue.

PLACE TABLE 3.3 ABOUT HERE; WIDTH = 1.5 COLUMNS

Calculating Mahalanobis' Distances

Before embarking on the drift/selection analyses, we first assessed differences and similarities between fossil specimens in the context of different models of extant variation by calculating Mahalanobis' distances (D^2) (Rohlf and Marcus 1993). The Mahalanobis' distance equation is denoted as follows:

$$D^2 = (x_1 - x_2)' V^{-1} (x_1 - x_2)$$

where D^2 equals the squared Mahalanobis' distance between specimen 1 and specimen 2, x_1 is the vector of interlandmark distances for specimen 1, x_2 is the vector of inter landmark distances for specimen 2 and V^{-1} is the inverse of the variance/covariance (V/CV) matrix of the extant specimens (Ackermann 2003; Ackermann 2009; Schroeder 2007; Schroeder 2015).

Mahalanobis' distances were calculated in MATHEMATICA ™ v 10.2. For each analysis, all possible pairwise distances between fossil specimens were calculated, using each of the three extant species V/CV matrices (*G. gorilla, P. troglodytes and H. sapiens*). All possible pairwise Mahalanobis' distances were also calculated for each extant species to determine whether the differences between individuals in the fossil sample were statistically significant. For each pairwise comparison, multiple Mahalanobis' distances (using V/CV matrices from each of the three extant species, respectively) were calculated, following Ackermann (2002; 2003; 2009) and Schroeder (2007; 2015). D^2 values were considered statistically significant if they fell outside of the 95th percentile of relevant extant sample.

(Table 3.4). In addition to facilitating evaluation of statistical significance, this approach also allows us to examine how the use of these different V/CV matrices affects the understanding of inter-individual differences in *Paranthropus*.

Principal Coordinate Analyses (PCoA) were conducted using pairwise Mahalanobis' distances to visualize relationships between fossil specimens in each analysis. PCoA illustrated individual differences by graphically depicting inter-individual dissimilarities. Each axis represents an eigenvalue that equates to the amount of variation "captured" by that axis. The first axis represents the largest amount of variation and the second axis represents the second greatest variation in any given data set (Buttigieg and Ramette 2014). Similarity (clustering) or dissimilarity between individuals can be judged by observing the locations of individual specimens on the PCoA plot. It should be borne in mind, however, that, because the Mahalanobis' distances were based on absolute inter-landmark distances, the first principal coordinate will be driven in large part by size differences. Only the fossil specimens were included in the PCoA plots of the fossils to provide a more detailed assessment of intra-group variability.

PLACE TABLE 3.4 ABOUT HERE; WIDTH = 1.5 COLUMNS

Genetic Drift: Testing of the Null Hypothesis

Tests developed from Lande's (Lande 1977; 1979; 1980) evolutionary quantitative genetic theory were then used to analyze the relative roles of genetic drift and selection within *Paranthropus* (cf. Ackermann and Cheverud 2004). We tested the neutral model of evolution using the following equation:

$$B_t = G(t / N_e)$$

where B_t is the between population (fossil sample) phenotypic V/CV matrix, t is the number of generations, G is the additive genetic V/CV matrix, and N_e is the given effective population size (Ackermann and Cheverud 2002; Ackermann and Cheverud 2004). G can be substituted with the phenotypic within group V/CV matrix (P; in our case, our extant comparative analogues). This substitution follows Cheverud's conjecture (1988), which states that G and P matrices are directly proportional to each other, allowing for the latter to substitute for the former, specifically in the case of morphological traits. Although this substitution has been the subject of some criticism in the past (e.g., Kruuk et al. 2008), a recent study by Sodini et al. (2018) provides further support for this conjecture in human populations. The residual covariance matrix from a MANOVA was used to correct for sex in our estimated *P* (traits as dependent variables and sex as an independent variable). Because t and N_e are constants for each comparison, we are left with the following relationship:

$$(B \propto W)$$

This study followed Ackermann and Cheverud's (2002; 2004) approach in which within-group covariance matrices were converted to reduced uncorrelated principal components (Ackermann and Cheverud 2004). Logged between-group eigenvalues (B), calculated as the variance among group mean differences between fossil samples, are regressed (by means of least squares regression) onto logged within-group eigenvalues (W), obtained from principal components calculated from the extant covariance matrices substituted as models for within-population variability. A proportional relationship ($B \propto W$), which is indicated when the regression slope does not differ significantly from 1.0, signals a failure to reject the null hypothesis of drift (Ackermann and Cheverud 2004). By contrast, a non-proportional relationship between *B* and *W*, which is indicated when the regression slope is significantly different from 1.0, results in rejection of the null hypothesis of drift. Rejection of the null

hypothesis of drift indicates that the relationships between the within- and between-groups eigenvalues are non-proportional and that non-random forces, such as natural selection, are likely to be at work (Ackermann and Cheverud 2004). It is important to highlight that failing to reject drift does not eliminate the chance that non-adaptive forces were acting, however it implies that any effects of these non-random processes cannot be separated from the effects of divergence due to drift.

There are a number of limitations with this approach. First, this approach cannot tease apart the intricate effects of both processes acting on species diversification over a long geological timescale. Second, as stated above, given the small sample sizes of fossil groupings, extant model V/CV (phenotypic) matrices were used as analogues to estimate fossil within-group variation. This is not an ideal solution as it violates the basic assumption of the linear regression procedure that variables (here principal component scores for both *W* and *B*) are independent (given the use of an extant model to calculate $|W|$, and fossils used to calculate $|B|$), however, it is an unavoidable in this context. The final limitation of this test is related to fragmentary fossils that affect the number of traits, thus making it a more conservative test, which makes it more challenging to reject drift. In light of this limitation, when a significant deviation from a slope of 1.0 is detected, a strong case for selection can be made. This test is therefore considered a conservative one.

Reconstruction Selection

If the null hypothesis of drift is rejected, indicating that selection (our alternative hypothesis) may be the driving force between the divergence of two populations/taxa, quantitative genetic theory (Lande and Arnold 1983) also provides an approach for reconstructing the pattern and magnitude of selection acting to differentiate populations. This methodological approach is determined by the following relationship:

$$\beta = G^{-1}[z_i - z_j]$$

where β is the differential selection vector (vector of selection gradients) summed over generations, G^{-1} is the inverse of the genetic V/CV matrix, and $[z_i - z_j]$ is the difference in means between species i and j, in this case the fossil species being compared, representing the evolutionary response to selection for each trait. Again, V/CV matrices from extant species were used as analogues to estimate fossil within-group variation (sex-corrected *P*, which was substituted for *G*; see above) (Ackermann 2002; 2003; 2009). The elements of the selection gradient can be either negative or positive, representing each trait's respective relationship with fitness (Lande and Arnold 1983). The magnitude of selection relies on estimated extant model V/CV matrices, and results should be interpreted with caution as extant model choice may change the interpretation of results (Ackermann 2003). All analyses were performed using R v3.2.4.

Results

Mahalanobis' Distances and Principal Coordinate Analysis

Mahalanobis' distances calculated for each analysis using *H. sapiens*, *P. troglodytes* and *G. gorilla* V/CV matrices can be accessed online via ZivaHub (https://doi.org/10.25375/uct.7837673.v1). In general, patterns of D^2 values are comparable across all three extant models, with slight deviations in the detection of statistical significance evaluated against the 95th percentile frequency distributions (given in the online dataset mentioned above). We provide further discussion about those cases in which the patterns deviate significantly using the approach outlined in the 'Methods' section above. Below we describe the PCoA plots based on the Mahalanobis' distances of a select set of analyses

(Cranial Analyses, 1, 2, and 6 and Mandibular Analysis 2), which were chosen because they have the largest sample sizes (greater than 4 specimens for the crania, and the largest of the two samples for the mandible) and are therefore the most informative. For simplicity, only the plots using human and gorilla matrices are presented in Fig. 3.4, to reflect the broadest phenotypic range of the models with chimpanzees being relatively intermediate.

Cranium

For Cranial Analysis 1, Mahalanobis' distances and PCoA plots of these values for the midface-maxilla region (Fig. 3.4 A and B) indicate that OH 5 (*P. boisei*) is significantly different from all the other *Paranthropus* specimens (all of which are *P. robustus* specimens), with DNH 7 the most distant. In addition, SK 83 is significantly different from the other two *P. robustus* specimens (also from Swartkrans), highlighting the variability in this Swartkrans *P. robustus* sample. This pattern contrasts with that found in *A. africanus* fossils (all of which are from Sterkfontein), which shows that all of the Sterkfontein specimens are more closely clustered (and not significantly different regardless of the extant V/CV matrix that is used to model variation). It is worth noting that DNH 7 is only statistically different from any of the Swartkrans specimens when the chimpanzee V/CV model of variation is employed; the differences are not significant when human (Fig. 3.4 (A)) and gorilla (Fig. 3.4 (B)) models of variation are used.

PLACE TWO PARTS OF FIGURE 3.4 ABOUT HERE; FULL PAGE WIDTH ON FACING PAGES

The analyses of the zygomatic and upper face region (Cranial Analysis 2) differs from the previous analysis in the following ways: (1) only a single individual from Swartkrans (SK 48) is included; (2) Sts 5 is included, but Sts 52 is excluded; and (3) KNM-ER 732 (*P. boisei* from Koobi Fora) is included. All of the individuals are significantly different from each

other under at least one model of variation. OH 5 stands out as being different from all other fossil specimens including KNM-ER 732, but this specimen is particularly distinct from Sts 5, (Fig. 3.4 (C and D)). In these analyses, the two *A. africanus* specimens from Sterkfontein are further apart in shape space than those of *Paranthropus* (Fig. 3.4 (C and D)). Interestingly, DNH 7 aligns most closely with the *A. africanus* specimen, Sts 71.

For the analysis of the temporal region (Cranial Analysis 6; Fig. 3.4 (E and F)), the greatest difference is between SK 48 and all other specimens. However, all of the specimens are significantly different from each other under at least one model of variation. It is important to note that, DNH 7 clusters most closely with the East African specimens, KNM-WT 17000 and KNM-ER 406.

Mandible

The Mahalanobis' distances and associated principal coordinate plots for the mandibular corpus analysis (Mandibular Analysis 2; Fig. 3.4 (G and H)) primarily indicate that DNH 7 and DNH 8 are statistically different from all other specimens, including each other, regardless of the model that is used to test significance. There are also some significant differences between some southern and eastern African specimens, and among East African specimens. Also, in contrast to the variability detected among the Swartkrans cranial specimens, mandibles from Swartkrans form a relatively tight cluster (Fig. 3.4 (G and H)).

Testing the Null Hypothesis of Genetic Drift

All analyses were performed twice, once using data transformed by the natural logarithm, and again using non-transformed interlandmark distances. Tests carried out on transformed data overwhelmingly failed to reject a null hypothesis of drift, possibly indicating that size is an

important factor in differentiating between groups. Therefore, below we only present results of tests carried out on non-standardized data.

Table 3.4 summarizes the results of the tests of genetic drift for the analyses of the cranium and mandible. For each of these comparisons, tests were performed using human, chimpanzee, and gorilla V/CV matrices to model within-species variation, and this amounted to a total of 72 tests. Seven out of 72 tests rejected drift, meaning that drift could not be rejected for 90% of these tests. This result indicates that divergence between these species for these morphological regions could be explained by neutral evolutionary forces, but not completely excluding selection (and other evolutionary pressures).

However, even when drift was rejected, it occurred under only a single extant model. For example, in Cranial Analysis 1, which focuses on the midface/maxilla region, diversification between *A. africanus* and *P. robustus* under a human model of variation is inconsistent with drift, indicating that selection may have played a role. For Cranial Analysis 6, the temporal region, results for the comparisons of *P. aethiopicus* and *P. robustus*, and *P. aethiopicus* and *A. africanus*, show a rejection of drift under a chimpanzee model of variation, and the *P. robustus* and *A. africanus* comparison drift is rejected using the gorilla model. Comparisons between *P. boisei* and *P. robustus* species for the palate region (Cranial Analysis 7) demonstrate a rejection of drift for the chimpanzee model of variation.

Mandibular Analyses 1 and 2 only included, *P. boisei* and *P. robustus*. The results for Mandibular Analysis 1 (ramus and corpus) reject drift under a human model of V/CV, whereas, in Mandibular Analysis 2 (corpus only), drift is rejected under a chimp model of variation. As Mandibular Analysis 2 has the largest fossil sample size of all analysis subsets (n=11), this test was also run using a fossil hominin V/CV, which did not result in a rejection of null hypothesis of drift (slope=1.04; p=0.89). Although the size of the fossil sample is

smaller than the minimum size required for estimating V/CV matrices, it is interesting to present alongside the results of the extant models.

In addition to these cases in which the null hypothesis of drift were rejected, some analyses have *p*-values between 0.05 and 0.10, which is important to highlight given the conservative nature of this test. For Cranial Analyses 2 & 3 (zygomatic and upper face regions) various comparisons have *p*-values between 0.05 and 0.10 (see Table 3.4). Cranial Analysis 4, designed to examine the relationship between three presumed females (DNH 7, KNM-ER 732 and Sts 5), resulted in a *p*-value of 0.07 for the comparison between *P. robustus* and *A. africanus* under a human model of variation.

PLACE TABLE 3.4 ABOUT HERE; WIDTH = 1.5 COLUMNS

Reconstruction of Selection Vectors

The results show that, for the majority of comparisons, drift cannot be rejected. This finding indicates that patterns of diversification within the genus *Paranthropus* (and between *Paranthropus* and *A. africanus*) are consistent with neutral (random) evolutionary forces. Nonetheless, as discussed earlier, there are seven comparisons (Table 3.4) for which drift was rejected, suggesting that, in these cases, selection may explain the variation between groups. For these comparisons, we reconstructed the selection vectors required to explain the morphological differentiation among *Paranthropus* taxa and between *Paranthropus* and *A. africanus* (Table 3.5; Figs, 3.5- 3.7).

The elements of the selection gradient required to produce *P. robustus* midfacial and maxillary morphological changes from *A. africanus* in cranial analysis 1 (Fig. 3.5 (A); Table 3.5) are moderately positive to weak for the height of the maxilla and general tooth

enlargement. The nasal aperture, length of the palate, and P4 (maxillary) enlargement are also moderately negative to weak. For the bulk of the traits in this region, the response to selection is consistent with the direction and magnitude of selection (pressures), indicating that these traits were the result of direct selection.

Rejections of drift occur in the temporal region (Cranial Analysis 6) between *P. aethiopicus* and *P. robustus* (Fig. 3.5 (B)), *P. aethiopicus* and *A. africanus* (Fig. 3.5 (C)), and *P. robustus* and *Au. africanus* (Fig. 3.5 (D)), respectively. The elements of the selection gradient required to produce *P. robustus* temporal morphological change from *P. aethiopicus* is strongly negative for the external auditory meatus (EAM) in both height and width, as well as surrounding regions (e.g., MFL – EMI, POR – MFM and MFL – AST) (Fig. 3.5 (B); Table 3.5). In addition, the elements of the selection gradient are strongly positive for POR – MFL and AST – POR. The response to the selection mentioned above is mostly consistent with the pattern of selection with the exception of MFL – AST, which responds in the opposite direction to selection, indicating that this trait is not under direct selection, but is instead influenced by correlated selection on other traits.

The reconstructed elements of the selection gradient required to produce *P. aethiopicus* temporal morphological change from *A. africanus* (Fig. 3.5 (C)) are negative for EAM width, POR – MFL, and AST – MFL. However, the gradients are positive for the superoinferior height of the EAM and surrounding areas of the temporal region. The response to selection is again mostly consistent with the direction of selection, with the exception of MFL – AST.

The elements of the selection gradient necessary to explain divergence between a *P. robustus* temporal region from *A. africanus* (Fig. 3.5 (D)) are strongly negative for EAM width and height, and MFL – AST, but strongly positive for the remainder of the temporal

region. The response to selection is generally negative to neutral, excluding POR – MFM (which is positive). Results indicate that morphological change is likely due to a mix of direct and correlated selection on other traits.

For the palate (Fig. 3.6), the null hypothesis of drift is rejected in the comparison of *P. boisei* and *P. robustus*. The elements of the selection gradient reconstructed for this comparison are strongly negative for both palate depth and length, with magnitudes exceeding that of any previously described gradients. Moderate to strong positive elements of the selection gradient are detected for width and depth of the hard palate region. Responses to selection are primarily positive, suggesting that none of the traits for which negative gradients were detected are under direct selection.

For Mandibular Analysis 1, which includes traits across the corpus and ramus, drift is rejected between *P. robustus* and *P. boisei*. The elements of the selection gradient (Fig. 3.7 (A); Table 3.5) are weak to strongly negative for general length (MEN – RAM POS; ALVB – GON; MEN – GON) and inferior ramus height (RAM POS – GON), and are strongly positive for ramus width (AJUNC – RAM POS; AJUNC – GON). It must be pointed out that the response to this force is opposite in direction for many of these traits, especially mandibular length, indicating that these traits are not under direct selection. In other words, if the coefficient of the selection gradient is negative for a particular traits, but the response of that trait is an increase in size, rather than a decrease in size, that indicates a correlated response to a positive coefficient acting elsewhere.

In Mandibular Analysis 2, which focuses on corpus traits, the elements of the selection gradient necessary to produce a *P. robustus* corpus from *P. boisei* (Fig. 3.7 (B); Table 3.5) are weak to strongly negative for superoinferior height, posterior corpus length, and M1 to M3 molar length. These negative elements of the selection gradients correspond

with the response to selection for these traits, indicating a general decrease in molar size and shortening of superioinferior corpus height. The elements of the selection gradient reconstructed for P_4 and M_2 length are weakly positive. All responses to these elements of the selection gradient in this analysis are in line with the direction of selection.

PLACE FIGURE 3.5 ABOUT HERE; WIDTH = 1 COLUMN

PLACE TABLE 3.5 ABOUT HERE; WIDTH = 1.5 COLUMNS

PLACE FIGURE 3.6 ABOUT HERE; WIDTH = 1 COLUMN

PLACE FIGURE 3.7 ABOUT HERE; WIDTH = 1.5 COLUMNS

Discussion/Conclusion

Past research on the morphology of *Paranthropus* has primarily concentrated on describing cranial morphology and determining phylogenetic relationships, with less focus on understanding the underlying drivers of inter- and intra-specific variation (e.g., Rak 1983, Kimbel 2006; Wood 2010; Wood and Schroer 2017). Moreover, most interpretations of the craniofacial morphology of *Paranthropus* have been contextualized within an adaptive framework, with little consideration of the role that random divergence (i.e., genetic drift) may have played in producing diversity. The goal of this research was to further understand intra- and inter- specific variation in the cranium and mandible of *Paranthropus* by exploring the evolutionary processes that have shaped craniofacial diversification in this genus. What follows is a discussion of the findings in the context of these research objectives.

For the Mahalanobis' distances, a few patterns stand out. First, the southern and eastern African materials were generally distinct. Second, in the cranial analyses, the southern African *P. robustus* individuals showed high levels of variation, sometimes differing from each other as much as individuals from other species depending on which extant species (i.e., human, chimp or gorilla) was used to model variation. However, *P. robustus* specimens were also relatively tightly clustered in the mandibular analyses. Third, the individuals from Drimolen, DNH 7 and DNH 8, extended the range of *P. robustus,* well beyond the range of both the eastern and southern African *Paranthropus* material in the mandibular analyses. These analyses both support the distinctiveness of *Paranthropus* taxa, and highlight the variability within *P. robustus.* However, some of these results could be influenced by the relatively larger sample sizes in *P. robustus*. Nonetheless, these results suggest that the affiliations DNH 7 and DNH 8 in particular deserve further consideration.

Turning to the drift/selection tests, the results indicated that, for the vast majority (90%) of comparisons, drift could not be rejected. This includes the morphological diversification of the three *Paranthropus* taxa from each other and from *A. africanus*. The results suggest that non-adaptive processes may have played a more important role than previously thought in the diversification of *Paranthropus* morphology, specifically as it relates to the morphology of the upper face, zygoma, basicranium, and tooth complexes. However, it is worth restating that, while these results are consistent with the explanation that morphological diversity in *Paranthropus* is the result of genetic drift, they do not rule out selection as a contributor to this diversification and, importantly, do not provide evidence *in favour* of the null hypothesis of genetic drift.

The null hypothesis of genetic drift was rejected in seven comparisons (representing ~9% of all tests; Table 3.4) across the following regions: midface, temporal region of the skull, the mandible (corpus, ramus and midline regions), and maxilla (including the hard

palate). These regions relate to the masticatory apparatus and are involved in feeding biomechanics. Thus, these results were consistent with adaptive/functional interpretations of *Paranthropus* morphology. The regions included those to which the muscles of mastication attach (i.e., the origin and/or insertion of the masseter, temporalis, and medial pterygoid muscles), as well as regions (e.g., the hard palate and mandibular corpus) that would be modified by natural selection to resist strains encountered during feeding on a diet including hard and/or tough foods. It is noteworthy, though, that the null hypothesis of drift was not rejected in analyses of other regions that also comprise the masticatory apparatus (e.g., parts of the zygoma). This finding suggests that strong directional selection may not have solely driven the evolution of all the morphological features that constituted the masticatory apparatus and may instead indicate that both evolutionary pressures have played a role in in lineage differentiation (Ackermann and Cheverud 2004). Further studies are required to disentangle the nuances of these results, as they are mixed, with regard to the degree to which the uniquely derived features of the genus *Paranthropus* are functional traits that were molded by natural selection as dietary adaptations.

Morphological responses to selection differed across the analyses in which drift was rejected. However, there are some noteworthy trends. For example, the results of most of the analyses (including different cranial and mandibular regions and ancestor-descendant pairs) were generally consistent insofar as they show morphology responded in concert with selection vectors (positive selection vector, increase in size response and vice versa), including for features such as maxillary height and overall tooth enlargement. However, for some traits, such as length and depth of the palate, traits in the temporal region (e.g., MFL – AST), and mandibular corpus length, changes in morphological features occurred in a direction opposite to selection. This result provides evidence for correlated responses to selection, which requires further investigation.

The relative effects of drift versus selection are not the same across all taxon comparisons. This inconsistency provides some insight into the different processes underlying morphological divergence in the three recognized *Paranthropus* taxa. It also offers the potential to improve our understanding of the phylogenetic relationships among these three species. Neutrality tests indicated that the null hypothesis, i.e. that genetic drift explains the differences between *P. aethiopicus* and *P. boisei,* cannot be rejected in any case. In contrast, tests for the diversification between *P. robustus* and the two eastern African species, *P. aethiopicus* and *P. boisei*, do not rule out adaptive divergence. In this case, both eastern African specimens are chronologically older with clear geographic differences. These results suggest that *P. aethiopicus* (the "Black Skull", KNM-ER 17000), dated to 2.53 Ma, a taxon that is chronologically older than, but in geological proximity (and possibly ancestral) to *P. boisei* (Strait et al. 1997), may have evolved into *P. boisei* through neutral processes. In contrast, diversification between *P. robustus* and the eastern African taxa may have occurred via a more complex adaptive path. These results are particularly interesting in light of recent stable isotope and dental microwear evidence that suggests that *P. boisei* and *P. robustus* ate different foods (Ungar et al. 2008; Rabenold and Pearson 2011; Sponheimer et al. 2013). Moreover, this finding provides evidence consistent with the idea that dietary differences were responsible for this adaptive differentiation, and that this differentiation is detectible in morphology. However, the fact that natural selection was not shown to drive the evolution of all the morphological features that constitute the masticatory apparatus might indicate that the masticatory complex (as a whole) is not directly targeted by selection in its entirety, but, rather, that the differences in the components of the complex may be the result of correlated selection that affects areas related to the masticatory complex.

In general, the results of this study suggest that direct selection may have played a more minor role in shaping the cranio-mandibular morphology within the genus

Paranthropus than previously thought. Instead, this study highlights the possible influence of non-adaptive evolutionary processes on the evolution and diversity of cranial and mandibular anatomy in this genus.

There are two important limitations to the study, both of which revolve around sample size and specimen preservation that should be mentioned. First, the samples of *Paranthropus* fossils, like those of all hominin taxa, are limited in number. In addition, many of the specimens are poorly preserved, distorted and/or fragmented. Small sample sizes and poor preservation (including crushing, matrix expansion etc.) generally result in less robust conclusions. Second, and more specifically, because of the small sample sizes, it is impossible to estimate within group variability (represented by a V/CV matrix) for *Paranthropus* with any accuracy (see Ackermann [2009]). This fact necessitates the use of extant species as models to estimate V/CV of fossil taxa, which is problematic given that V/CV matrices of even closely related species can differ in magnitude (and sometimes pattern) (Ackermann 2002; Ackermann 2003; Ackermann 2005). Here, an attempt was made to minimize these problems—i.e., multiple comparative extant samples were used as models for estimating of within-taxon variation in *Paranthropus.* In addition, the drift/selection test for Mandibular Analysis 2 was run using a fossil hominin V/CV matrix (with a sample size of n=11). Nevertheless, in the absence of large samples of *Paranthropus* fossils, there is no obviously appropriate analogue for the morphological variability in this highly derived genus. This unavoidable limitation is also clearly reflected in the variability of the results depending on the extant model that was employed and the apparent lack of any patterning in the results in this regard (e.g., none of the analyses had consistent rejection of drift across all extant taxa (Table 3.4)).

There are a number of avenues for future research. Although the results described here suggest that selection was responsible for shaping some of the morphological regions

that are related to the masticatory apparatus, it is unclear why selection was *not* implicated in the morphology of other regions that are also related to feeding behavior. Although it is also not entirely clear why certain aspects of morphology changed in the direction of selection, whereas other changes occurred in the opposite direction as a result of correlated selection, this phenomenon is likely due to the underlying architecture of the unknown taxon-specific variance/covariance structure(s). Future research is needed to further understand these nuances, as well as test hypotheses related to adaptive diversification across *Paranthropus* that more directly address questions about functional morphology and mastication (and biomechanics related to functional capabilities) linked to diet.

Acknowledgments

We would like to thank Bernard Wood and Paul Constantino for the opportunity to contribute to this book, and to participate in the symposium on which this special issue was based. We would like to the thank National Research foundation of South Africa (NRF), Centre of Excellence in Paleosciences (CoE-Pal), and Palaeontological Scientific Trust (PAST) Research Grant for funding this research project. We would like to thank Dr Lynn Copes for contributing her primate scans for this research. Thank you for the scans collected by Jesse Martin, Angeline Leece and Dr. Andy Herries (La Trobe University) funded by the Australian Research Council Discovery Grant through The Australian Archaeomagnetism Laboratory and a Society of Antiquaries of London grant to Jesse Martin that allowed them to conduct this research towards the Drimolen specimens. We would also like to thank the Smithsonian's Division of Mammals (Dr. Kristofer Helgen) and Human Origins Program (Dr. Matt Tocheri) for the scans of USNM specimens used in this research. These scans were acquired through the generous support of the Smithsonian 2.0 Fund and the Smithsonian's

Care and Preservation Fund. We are grateful to the many institutions and individuals for access to fossil and extant primate and human materials in their care: E. Mbua, P. Kiura, and the National Museums of Kenya; the National Museum and House of Culture of Tanzania; S. Potze and the Ditsong Museum; B. Billings and the School of Anatomical Sciences of the University of the Witwatersrand; B. Zipfel and the Evolutionary Studies Institute at the University of the Witwatersrand; W. Seconna of the Iziko South African Museum; and Y. Haile-Selassie and L.M. Jellema of the Cleveland Museum of Natural History.

Supplementary Online Material

Supplementary Online Material pertaining to this chapter can be found at https://doi.org/10.25375/uct.7837673.v1.

References

Ackermann, R.R. (1998). A quantitative assessment of variability in the australopithecine, human, chimpanzee and gorilla face. Ph.D. Dissertation, University of Washington, St. Louis.

Ackermann, R.R. (2002). Patterns of covariation in the hominoid craniofacial skeleton: implications for paleoanthropological models. *Journal of Human Evolution*, *42*(1), 167-187.

Ackermann, R.R. (2003). Using extant morphological variation to understand fossil relationships: a cautionary tale. *South African Journal of Science*, *99*(1), 255-258.

Ackermann, R.R. (2005). Variation in Neanderthals: a response to Harvati (2003). *Journal of Human Evolution*, *48*(6), 1-4.

Ackermann, R.R. (2009). Morphological integration and the interpretation of fossil hominin diversity. *Evolutionary Biology*, *36*(1), 149-156.

Ackermann, R.R., & Cheverud, J.M. (2002). Discerning evolutionary processes in patterns of tamarin (genus *Saguinas*) craniofacial variation. *American Journal of Physical Anthropology*, *117*(3), 260-271.

Ackermann, R.R., & Cheverud, J.M. (2004). Detecting genetic drift versus selection in human evolution. *PNAS, 101*(52), 17946-17951.

Arnold, M.L. (1992). Natural hybridization as an evolutionary process. *Annual review of Ecology and Systematics, 23*(1), 237-261.

Bass, W.M. (1987). *Human osteology: A laboratory and field manual (No. 2).* Springfield: Missouri Archaeological Society.

Broom, R. (1938b). The Pleistocene anthropoid apes of South Africa. *Nature*, *142*(3591), 377-379.

Buttigieg, P.L., & Ramette, A. (2014). A guide to statistical analysis in microbial ecology: a community-focused, living review of multivariate data analyses. *FEMS Microbiology Ecology*, *90*(3), 543–550.

Cheverud, J.M. (1988). A comparison of genetic and phenotypic correlations. *Evolution, 42*(5), 958-968.

Cerling, T.E., Mbua, E., Kirera, F.M., Manthi, F.K., Grine, F.E., Leakey, M.G., et al. (2011). Diet of *Paranthropus boisei* in the early Pleistocene of East Africa. *Proceedings of the National Academy of Sciences*, *108*(23), 9337-9341.

Copes, L.E. (2012). Comparative and experimental investigations of cranial robusticity in mid-Pleistocene hominins. Ph.D. Dissertation, Arizona State University.

Copes L.E., & Kimbel, W.H. (2016). Cranial vault thickness in primates: *Homo erectus* does not have uniquely thick vault bones. *Journal of Human Evolution, 90*(1), 120-134.

Freidline, S.E., Gunz, P., Harvati, K., & Hublin, J.J. (2012). Middle Pleistocene human facial morphology in an evolutionary and developmental context. *Journal of Human Evolution, 63*(5), 723-740.

Hlazo, N. (2015). Paranthropus*: variation in cranial morphology.* Honours Thesis, University of Cape Town.

Hlazo, N. (2018). *Variation and the evolutionary drivers of diversity in the genus* Paranthropus. Master's Thesis, University of Cape Town.

Kimbel, W.H. (2006). The species and diversity of australopiths. In W. Henke & I. Tattersall (Eds.), *Handbook of paleoanthropology* (pp. 1-30). Berlin, Heidelberg: Springer.

Kimura, M. (1968). Evolutionary rate at the molecular level. *Nature*, *217*(1), 624-626.

Kimura, M. (1991). The neutral theory of molecular evolution: a review of recent evidence. *The Japanese Journal of Genetics, 66*(4), 367-386.

Kruuk, L.E., Slate, J., & Wilson, A.J. (2008). New answers for old questions: the evolutionary quantitative genetics of wild animal populations. *Annual Review of Ecology, Evolution, and Systematics, 39*(1), 525-548.

Lande, R. (1976). Natural selection and random genetic drift in phenotypic evolution. *Evolution, 30*(2), 311-334.

Lande, R. (1977). Statistical tests for natural selection on quantitative characters. *Evolution, 31*(2), 442-444.

Lande, R. (1979). Quantitative genetic analysis of multivariate evolution: applied to brain:body size allometry. *Evolution, 33*(1), 402-416.

Lande, R. (1980). Genetic variation and phenotypic evolution during allopatric speciation. *The American Naturalist, 116*(4), 463-479.

Lande, R., & Arnold, S.J. (1983). The measurement of selection on correlated characters. *Evolution, 37*(6), 1210-1226.

Leakey, R.E.F., & Walker, A. (1988). New *Australopithecus boisei* specimens from East and West Lake Turkana, Kenya. *American Journal of Physical Anthropology, 76*(1), 1-24.

Lofsvold, D. (1988). Quantitative genetics of morphological differentiation in *Peromyscus* II. Analysis of selection and drift. *Evolution, 42*(1), 54-67.

Lucas, P.W., Omar, R., Al-Fadhalah, K., Almusallam, A.S., Henry, A.G., Michael, S., et al. (2013) Mechanisms and causes of wear in tooth enamel: implications for hominin diets. *Journal of the Royal Society Interface, 10*(1), 1-9.

Marriog, G., & Cheverud, J. M. (2004). Did natural selection or genetic drift produce the cranial diversification of neotropical monkeys? *The American Naturalist, 163*(3), 417-428.

Martinez, L.M., Estebaranz-Sάnchez, F., Galbany, J., & Pérez-Pérez, A. (2016). Testing dietary hypotheses of East African hominins using buccal dental microwear data. *PLOS ONE, 11*(11), 1-25.

McCollum, M.A. (1999). The robust australopithecine face: a morphogenetic perspective. *Science, 284*(1), 301-304.

Rabenold, D., & Pearson, O.M. (2011). Abrasive, silica phytoliths and the evolution of thick molar enamel in primates, with implications for the diet of *Paranthropus boisei*. *PLOS ONE, 6*(12), 1-11.

Rak, Y. (1983). *The australopithecine face*. New York: Academic Press.

Rohlf, F.J., & Marcus, L.F. (1993). A revolution morphometrics. *Trends in Ecology & Evolution, 8*(4), 129-132.

Roseman, C.C. (2004). Detecting interregionally diversifying natural selection on modern human cranial form by using matched and morphometric data. *Proceedings of the National Academy of Sciences of the United States of America, 101*(35), 12824-12829.

Schroeder, L. (2007). Using Mahalanobis' generalised distances to investigate morphological relationships and variation in early Homo dental specimens. Honours Thesis, University of Cape Town.

Schroeder, L. (2015). The evolution and diversification of Pleistocene *Homo.* Ph.D. Dissertation, University of Cape Town.

Schroeder, L., & Ackermann, R.R. (2017). Evolutionary processes shaping diversity across the *Homo* lineage. *Journal of Human Evolution, 111*(1), 1-17.

Schroeder, L., & von Cramon-Taubadel, N. (2017). The evolution of hominoid cranial diversity: a quantitative genetic approach. *Evolution, 71*(11), 2634-2649.

Schroeder, L., Roseman, C.C., Cheverud, J.M., & Ackermann, R.R. (2014). Characterizing the evolutionary path(s) to early *Homo*. *PLOS ONE*, *9*(2), 1-20.

Smith, A.L., Benazzi, S., Ledogar, J.A., Tamvada, K., Pryor Smith, L.C., Weber, G.W., et al. (2015). The feeding biomechanics and dietary ecology of *Paranthropus boisei. The Anatomical Record, 298*(1), 145-167.

Sponheimer, M., Alemsged, Z., Cerling, T.E., Grine, F.E., Kimbel, W.H., Leakey, M.G., et al. (2013). Isotopic evidence of early hominin diets. *Proceedings of the National Academy of Sciences, 110*(6), 10513-10518.

Stansfield, E., & Gunz, P. (2011). Skhodnya, Khvalynsk, Satanay, and Podkumok calvariae: possible Upper Paleolithic hominins from European Russia. *Journal of Human Evolution, 60*(1), 129-144.

Sodini, S.M., Kemper, K.E., Wray, N.R., & Trzaskowski, M. (2018). Comparison of genotypic and phenotypic correlations: Cheverud's conjecture in humans. *Genetics, 209*(3), 941-948.

Strait, D.S., Grine, F.E., & Moniz, M.A. (1997). A reappraisal of early hominid phylogeny. *Journal of Human Evolution, 32*(1), 17-82.

Ungar, P.S., & Sponheimer, M. (2011). The diets of early hominins. *Science, 334*(1), 190-193.

Ungar, P.S., Grine, F.E., & Teaford, M.F. (2008). Dental microwear and diet of the Plio-Pleistocene hominin *Paranthropus boisei*. *PLOS ONE, 3*(4), 1-6.

von Cramon-Taubadel, N., & Smith, H.F. (2012). The relative congruence of cranial and genetic estimates of hominid taxon relationships: implications for the reconstruction of hominin phylogeny. *Journal of Human Evolution, 62*(1), 640-653.

Weaver, T.D., Roseman, C.C., & Stringer, C.B. (2007). Were Neandertal and modern human cranial differences produced by natural selection or genetic drift? *Journal of Human Evolution, 53*(2), 135-145.

Williams, F.L. (2015). Dietary proclivities of *Paranthropus robustus* from Swartkrans, South Africa. *Anthropological Review, 78*(1), 1-19.

Wood, B.A. (2010). Reconstructing human evolution: achievements, challenges, and opportunities. *Proceedings of the National Academy of Sciences, 10*(2), 8902-8909.

Wood, B., & Schroer, K. (2013). *Paranthropus*. In D. Begun (Ed.), *Companion to palaeoanthropology* (pp. 457–478). New York: Wiley-Blackwell.

Wood, B., & Schroer, K. (2017). *Paranthropus*: where do things stand? In A. Marom & E. Hovers (Eds.), *Human palaeontology and prehistory*. New York: Springer.

Table 3.1. Fossil and Comparative samples in the study.

Species	Specimen	Museum
Paranthropus aethiopicus	2	Kenya National Museums west Turkana, National Museums of Kenya, Nairobi
		Kenya National Museums east Rudolf, National Museums of Kenya, Nairobi
Paranthropus boisei	10	OH (Olduvai hominin), National Museum of Tanzania, Dar es Salaam
		Drimolen, University of the Witswatersrand, Johannesburg, South Africa
Paranthropus robustus	27	Swartkrans, Ditsong National Museum of Natural History, Pretoria, South Africa
		Swartkrans, University of Witswatersrand, Johannesburg, South Africa
Australopithecus africanus	3	Sterkfontein, Ditsong National Museum of National History, Pretoria, South Africa
Homo sapiens	100	Raymond Dart Collection, University of Witswatersrand, Johannesburg, South Africa
		Iziko Museums of South Africa, Cape Town, South African
		Terry Collection, Smithsonian Collection and Human Origins Program, Washington D.C., Washington
		Duke University, Evolutionary Anthropology in Durham, North Carolina
Pan troglodytes	93	Hamann-Todd Collection at the Cleveland Museum of Natural History in Cleveland, Ohio
		Duke University, Evolutionary Anthropology in Durham, North Carolina
		Museum of Comparative Zoology in Harvard University in Cambridge, Massachusetts
		Smithsonian Institute, Smithsonian National Museum of Natural History, Washington D.C., Washington
Gorilla gorilla	100	Hamann-Todd Collection at the Cleveland Museum of Natural History in Cleveland, Ohio

Table 3.2. Cranial and mandibular landmarks recorded on specimens analyzed in this study. Landmarks are visualized in Fig. 3.2. [1, 2]

Cranial			
	Landmark Abbreviation	**Landmark**	**Landmark Description**
1	FMT	Frontomalare temporale	The most lateral point on the frontozygomatic suture
2	GLA	Glabella	Most anterior midline point on the frontal bone
3	NA	Nasion	The point at the intersection of the nasofrontal suture and the midsagittal plane
4	OR	Orbitale	The most inferior point on the midpoint of the lower edge of the orbit
5	DAC	Dacryon	The point of intersection of the frontolacrimal and lacrimomaxillary sutures
6	ZS	Zygomaxillare superior	The most superior point on the zygomaticotemporal suture
7	ZI	Zygomaxillare inferior	The most inferior point on the zygomamaxillary suture
8	OPH	Ophryon	Midline of the forehead immediately above the orbits
9	MF	Maxillofrontale	The point of intersection of the anterior lacrimal crest (medial edge of eye orbit), or the crest extended, with the frontomaxillary suture
10	IOF	Infraorbital foramen	The most inferior lateral point on the border of the infraorbital foramen
11	ALR	Alare	The most lateral point on the nasal aperture
12	ANS	Anterior Nasal spine	The most anterior midpoint of the anterior nasal spine of the maxilla
13	PRO	Prosthion	The most anterior point in the midline of the maxillary alveolar process
14	OL	Orale	The point where a line drawn tangent to the inner margin of the sockets of the two middle incisors of the upper jaw and projected onto the hard palate intersects the midsagittal plane
15	ENM	Endomalare	The most medial point on the inner surface of the alveolar ridge
16	ZTI	Zygotemporale inferior	The most inferior point on the zygomaticotemporal suture
17	ZTS	Zygotemporale superior	The most superior point on the zygomaticotemporal suture
18	POR	Porion	The most superior point on the margin of the external auditory meatus
19	EAM (A)	Ext auditory meatus	The most anterior point on the margin of the external auditory meatus
20	EAM (P)	Ext auditory meatus	The most posterior point on the margin of the external auditory meatus
21	EMI	External auditory meatus inferior	The most inferior point on the margin of the external auditory meatus
22	MAS	Mastoidale	The most inferolateral point on the mastoid process
23	AST	Asterion	The junction of the lambdoid, parietomastoid and occipitomastoid sutures
24	HOR	Hormion	The midpoint junction of the posterior aspect of the vomer and sphenoid bone
25	BA	Basion	The midpoint on the anterior border of the foramen magnum
26	OCA (A)	Occipitocondyle anterior	The most anteroinferior point on the occipital condyle
27	MFL	Lateral mandibular fossa	The most lateral point on the mandibular fossa
28	MFM	Medial mandibular fossa	The most medial point on the mandibular fossa
29	P3D	Distal P3	The most distal point on P3
30	P4D	Distal P4	The most distal point on P4/The most mesial point on M1
31	M1D	Distal M1	The most distal point on M1/The most mesial point on M2
32	M2D	Distal M2	The most distal point on M2/The most mesial point on M3
33	M3D	Distal M3	The most distal point on M3
34	IDS	Infradentale superius (alveolare)	The upper alveolar point; the apex of the septum between the upper central incisors
35	OL	Orale	The point where a line drawn tangent to the inner margin of the sockets of the two middle incisors of the upper jaw and projected onto the hard palate intersects the midsagittal plane
36	INC	Incisivon	The most posteroinferior point on the border of the incisive foramen
37	PTM	Palatomaxillare	The midline point of intersection of the palatine and the maxillary bones
38	ALV	Alveolon	The intersection of the interpalatal suture and a line tangent to the posterior margins of the alveolar processes
39	M3DL	Distal/Lingual M3	The most distal point on the inner lingual surface of the alveolar ridge on M3
40	M2DL	Distal/Lingual M2	The most medial point on the inner surface of the alveolar ridge between M3 and M2
41	P3DL	Distal/Lingual P3	The most medial point on the inner surface of the alveolar ridge between P4 and P3
42	M3DB	Distal/Buccal M3	The most distal point on the outter buccal surface of the alveolar ridge on M3
43	M2DB	Distal/Buccal M2	The most lateral point on the outter surface of the alveolar ridge between M3 and M2
44	P3DB	Distal/Buccal P3	The most lateral point on the outter surface of the alveolar ridge between P4 and P3

		Mandibular	
1	AJUNC	Inferior anterior ramus	The junction of the anterior border of the ramus and alveolus;
			The most anterior point on the ascending ramus in line with the alveolus
2	GON	Gonian	The point of maximum curvature on the posterior-inferior border
			where the posterior ramus and the corpus intersect
3	MEN	Mental foramen	The most anteroinferior edge of the mental foramen
4	ALVB	Alveolar border of body	The most superior point on the alveolus directly above the mental foramen
5	IBB	Inferior border of body	The most inferior point on the mandibular corpus directly below the mental foramen
6	RAM POS	Ramus posterior	The most posterior point on the ascending ramus in line with the alveolus
7	P3D	Distal P3	The most distal point on P3
8	P4D	Distal P4	The most distal point on P4/The most mesial point on M1
9	M1D	Distal M1	The most distal point on M1/The most mesial point on M2
10	M2D	Distal M2	The most distal point on M2/The most mesial point on M3
11	M3D	Distal M3	The most distal point on M3
12	ALVS	Alveolus	The most superior,posterior point on the alveolus

[1]Landmarks adapted from Bass 1987; Freidline et al. 2012; Schroeder 2015; Stansfield and Gunz 2011; Von Cramon-Taubadel and Smith 2012.

[2] Interlandmark distances were extracted from these landmarks as follows:

GLA-OPH; GLA-NA; NA-MF; MF-GLA; NA-FMT; DAC-FMT; FMT-ZI; ZI-OR; ZS-ZI; ZI-IOF; DAC-ALR; ANS-ALR; ANS-PRO; DAC-NA; PRO-ZTI; ZTS-ZTI;EMI-ZTI; POR-EMI; POR-MFL; POR-MFM; AST- POR; MFL-AST; ZTI-MFL; MFL-MFM; EAM (P)- EAM (A); POR-MAS; HOR-BA; HOR- MFL; OCA (A)-BA; BA-AST;EMI-OCA (A); MFM-EMI; MFL-EMI; EMI-HOR; MEN-RAM POS; AJUNC-RAM POS; AJUNC-GON; ALVS –GON; RAM POS-GON; MEN-GON; MEN-ALVB; MEN-IBB; P3D-P4D; P4D-M1D;M1D-M2D; M2D-M3D; ALVB-M2D; ENM-OL; IDS-OL; IDS-INC; IDS-PTM; IDS-ALV; OL-INC; OL-PTM; OL-ALV; INC-PTM; INC-ALV; PTM-ALV;ALV-M 3DL; ALV-M3DB; PTM-M2DL; PTM-M2DB; INC-P3DL; INC-P3DB.

Table 3.3. Sub-sets of analyses and inter-landmark distances in this study.

Analysis	Regions	Fossil Specimens	*G. gorilla*	*P. troglodytes*	*H. sapiens*	Inter-landmark Distance
Cranial Analysis 1	Midface-maxilla	OH 5, SK 46, SK 79, SK 83, DNH 7, Sts 52, Sts 71	49	48	45	ANS-PRO, ALR-ANS, P3D-P4D, P4D-M1D, M1D-M2D, M2D-M3D, ENM-OL
Cranial Analysis 2	Zygomatic	KNM-ER 732, OH 5, SK 48, DNH 7, Sts 5, Sts 71	49	46	50	ZS-ZI, ZI-IOF, OR-ZI, ZTS-ZTI, ZI-FMT
Cranial Analysis 3	Zygomatic-Upper face	KNM-ER 406, SK 48. Sts 5, Sts 71	50	45	50	GLA-NA, DAC-ALR, ZTS-ZTI, DAC-FMT, NA-FMT, MF-FLA, NA-MF, PRO-ZTI, DAC-NA, ZTI-MFL, ZTI-EMI
Cranial Analysis 4	Upper face-Temporal	KNM-ER 732, DNH 7, Sts 5	49	46	50	OPH-GLA, ZS-ZI, ZI-IOF, OR-ZI, ZTS-ZTI, ZI-FMT, POR-MAS
Cranial Analysis 5	Basicranium	KNM-WT 17000, KNM-ER 406, Sts 5	47	46	50	MFL-MFM, BA-HOR, HOR-MFL, OCA (A)-BA, AST-BA [L], EMI-OCA (A), MFM-EMI, EMI-HOR
Cranial Analysis 6	Temporal	KNM-WT 17000, KNM-ER 406, SK 48, DNH 7, Sts 5	50	50	50	EAM (A)-EAM (P), EMI-POR, MFL-EMI, POR-MFL, POR-MFM, AST-POR [L], MFM-AST
Cranial Analysis 7	Palate	SK 48, SK 79, OH 5	45	41	50	IDS-OL, IDS-INC, IDS-PTM, IDS-ALV, OL-INC, OL-PTM, OL-ALV, INC-PTM, INC-ALV, PTM-ALV, ALV-M3DL, ALV-M3DB, PTM-M2DL, PTM-M2DB, INC-P3DL, INC-P3DB
Mandibular Analysis 1	Ramus and Corpus	KNM-ER 729, SK 12, SK 23, SK 34	50	43	50	MEN-RAM POS, AJUNC-RAM POS, AJUNC-GON, ALVS-GON, RAM POS- GON, MEN-GON
Mandibular Analysis 2	Corpus	KNM-ER 403, KNM-ER 729, KNM-ER 3230, SK 12, SK 23. SK 34, SK 81, SK 876, SKW 5, DNH 7, DNH 8	50	42	49	MEN-ALVB, MEN- IBB, P3D-P4D, P4D-M1D, M1D-M2D, M2D-M3D, ALVB-M2D

Table 3.4. The cranial and mandibular regions analysed are listed in the first column, different species compared for each region listed in the next column (divergence in terms of ancestor tested), and whether there is a rejection of drift in the third column. The model of which rejection of drift listed in the second to last column followed by its p-value and R^2.

ANALYSIS	COMPARISON	REJECTION OF DRIFT?	MODEL	P-VALUE	R^2
CRANIAL ANALYSIS 1 MIDFACE/MAXILLA					
	P. boisei-P. robustus	NO	HUMAN	0.71	0.55
	P. boisei-P. robustus	NO	CHIMP	0.4	0.69
	P. boisei-P. robustus	NO	GORILLA	0.6	0.57
	P. boisei-A. africanus	NO	HUMAN	0.45	0.44
	P. boisei-A. africanus	NO	CHIMP	0.4	0.26
	P. boisei-A. africanus	NO	GORILLA	0.36	0.08
	A. africanus- P. robustus	YES	HUMAN	**0.04**	0.07
	A. africanus- P. robustus	NO	CHIMP	0.7	0.55
	A. africanus- P. robustus	NO	GORILLA	0.16	0.54
CRANIAL ANALYSIS 2 ZYGOMATIC					
	P. boisei-P. robustus	NO	HUMAN	0.22	0.75
	P. boisei-P. robustus	NO	CHIMP	0.66	0.26
	P. boisei-P. robustus	NO	GORILLA	0.57	0.06
	P. boisei-A. africanus	NO	HUMAN	0.77	0.71
	P. boisei-A. africanus	NO	CHIMP	0.45	0.17
	P. boisei-A. africanus	MAYBE	GORILLA	**0.09**	0.9
	A. africanus- P. robustus	NO	HUMAN	0.99	0.17
	A. africanus- P. robustus	NO	CHIMP	0.23	0.09
	A. africanus- P. robustus	NO	GORILLA	0.9	0.62
CRANIAL ANALYSIS 3					

ZYGOMATIC-UPPER FACE					
	P. boisei-P. robustus	NO	HUMAN	0.75	0.72
	P. boisei-P. robustus	MAYBE	CHIMP	**0.1**	0.61
	P. boisei-P. robustus	NO	GORILLA	0.75	0.43
	P. boisei-A. africanus	NO	HUMAN	0.5	0.42
	P. boisei-A. africanus	NO	CHIMP	0.86	0.5
	P. boisei-A. africanus	NO	GORILLA	0.73	0.53
	A. africanus- P. robustus	MAYBE	HUMAN	**0.09**	0.6
	A. africanus- P. robustus	MAYBE	CHIMP	**0.06**	0.46
	A. africanus- P. robustus	NO	GORILLA	0.75	0.43
CRANIAL ANALYSIS 4 FEMALES					
	P. boisei- P. robustus	NO	HUMAN	0.89	0.01
	P. boisei- P. robustus	NO	CHIMP	0.26	0.06
	P. boisei- P. robustus	NO	GORILLA	0.38	0.02
	P. boisei-A. africanus	NO	HUMAN	0.92	0.45
	P. boisei-A. africanus	NO	CHIMP	0.76	0.02
	P. boisei-A. africanus	NO	GORILLA	0.11	0.21
	P. robustus-A. africanus	MAYBE	HUMAN	**0.07**	0
	P. robustus-A. africanus	NO	CHIMP	0.87	0.09
	P. robustus-A. africanus	NO	GORILLA	0.15	0.07
CRANIAL ANALYSIS 5 BASICRANIUM					
	P. aethiopicus - P. boisei	NO	HUMAN	0.15	0.59
	P. aethiopicus - P. boisei	NO	CHIMP	0.79	0.55
	P. aethiopicus - P. boisei	NO	GORILLA	0.26	0
	P. aethiopicus - A.africanus	NO	HUMAN	0.32	0.15
	P. aethiopicus - A. africanus	NO	CHIMP	0.78	0.25
	P. aethiopicus - A. africanus	NO	GORILLA	0.82	0.19

	P. boisei-Africanus	NO	HUMAN	0.82	0.45
	P. boisei-Africanus	NO	CHIMP	0.87	0.62
	P. boisei-Africanus	NO	GORILLA	0.46	0.18
CRANIAL ANALYSIS 6 TEMPORAL					
	P. aethiopicus - P. boisei	NO	HUMAN	0.93	0.59
	P. aethiopicus - P. boisei	NO	CHIMP	0.65	0.28
	P. aethiopicus - P. boisei	NO	GORILLA	0.14	0.56
	P. aethiopicus- P. robustus	NO	HUMAN	0.61	0.25
	P. aethiopicus- P. robustus	YES	CHIMP	**0.05**	0.04
	P. aethiopicus- P. robustus	NO	GORILLA	0.18	0.43
	P. aethiopicus- A .africanus	NO	HUMAN	0.32	0.56
	P. aethiopicus- A. africanus	YES	CHIMP	**0.02**	0
	P. aethiopicus- A. africanus	NO	GORILLA	0.37	0.34
	P. boisei-P. robustus	NO	HUMAN	0.8	0.34
	P. boisei-P. robustus	NO	CHIMP	0.18	0.48
	P. boisei-P. robustus	NO	GORILLA	0.54	0.26
	P. boisei-A. africanus	NO	HUMAN	0.37	0.73
	P. boisei-A. africanus	NO	CHIMP	0.79	0.22
	P. boisei-A. africanus	NO	GORILLA	0.32	0.31
	P. robustus- A. africanus	MAYBE	HUMAN	**0.1**	0
	P. robustus- A. africanus	NO	CHIMP	0.18	0.02
	P. robustus- A. africanus	YES	GORILLA	**0.01**	0.1
CRANIAL ANALYSIS 7 PALATE					
	P. boisei-P. robustus	NO	HUMAN	0.55	0.55
	P. boisei-P. robustus	YES	CHIMP	**0.01**	0.48
	P. boisei-P. robustus	MAYBE	GORILLA	**0.1**	0.52
MANDIBULAR ANALYSIS 1					

RAMUS AND CORPUS					
	P. boisei - P. robustus	YES	HUMAN	**0.01**	0.49
	P. boisei - P. robustus	NO	CHIMP	0.44	0.05
	P. boisei - P. robustus	NO	GORILLA	0.29	0.33
MANDIBULAR ANALYSIS 2 CORPUS					
	P. boisei - P. robustus	NO	HUMAN	0.92	0.08
	P. boisei - P. robustus	YES	CHIMP	**0.05**	0.04
	P. boisei - P. robustus	NO	GORILLA	0.32	0.07

Table 3.5. Reconstructed differential selection gradient vectors for the cranial and mandibular analyses.

CRANIAL ANALYSIS 1								
MIDFACE-MAXILLA		ANS-PRO	ALR-ANS	P3D-P4D	M2D-M1D	M1D-P4D	M2D-M3D	ENM-OL
A. africanus- P. robustus	DIFFERENCE VECTOR	4.30	-4.60	-0.50	-1.47	0.64	-1.56	-5.47
	β_h	0.26	-0.23	**-1.90**	0.00	*1.77*	0.05	-0.79
	β_c	0.70	-0.33	-0.04	**-2.27**	*3.12*	-0.45	**-1.56**
	βg	0.50	-0.61	**-1.67**	-0.98	*1.79*	0.05	-0.02
CRANIAL ANALYSIS 6		EAM (A)-EAM (P)	EMI-POR	MFL-EMI	POR-MFL	POR-MFM	AST-POR [L]	MFL-AST
TEMPORAL *P. aethiopicus-P. robustus*	DIFFERENCE VECTOR	**-1.34**	**-8.67**	**-4.03**	*4.85*	**-3.58**	*9.01*	*9.51*
	β_h	0.66	**-2.59**	*2.90*	*12.55*	-0.96	*12.38*	**-12.78**
	β_c	**-5.1**	**-6.39**	**-6.17**	*11.80*	**-2.54**	*3.06*	**-3.30**
	βg	-0.31	-0.83	0.67	**10.23**	-0.87	**9.70**	**-9.83**
CRANIAL ANALYSIS 6		EAM (A)-EAM (P)	EMI-POR	MFL-EMI	POR-MFL	POR-MFM	AST-POR [L]	MFL-AST
TEMPORAL *P. aethiopicus-A. africanus*	DIFFERENCE VECTOR	-3.11	2.35	4.86	-4.96	7.03	7.56	3.89
	β_h	-0.54	**-3.01**	*3.35*	**-4.81**	*3.11*	**-1.31**	*1.03*
	β_c	**-1.15**	2.24	*7.40*	**-7.65**	*4.03*	*1.84*	**-2.22**
	βg	0.34	**-1.69**	*1.88*	**-3.51**	*1.42*	0.12	0.29
CRANIAL ANALYSIS 6		EAM (A)-EAM (P)	EMI-POR	MFL-EMI	POR-MFL	POR-MFM	AST-POR [L]	MFL-AST
TEMPORAL *P. robustus- A. africanus*	DIFFERENCE VECTOR	-4.46	-6.32	0.83	-0.10	3.45	-1.46	-5.63
	β_h	0.12	**-5.61**	*6.20*	*7.74*	*2.15*	*11.07*	**-11.75**
	β_c	**-6.25**	**-4.15**	*1.31*	*4.14*	*1.48*	*4.91*	**-5.52**
	βg	0.04	**-2.53**	*2.57*	*6.72*	0.55	*9.82*	**-9.53**

CRANIAL ANALYSIS 7								
PALATE		IDS-OL	IDS-INC	IDS-PTM	IDS-ALV	OL-INC	OL-PTM	OL-ALV
P. boisei-P. robustus	DIFFERENCE VECTOR	0.63	1.41	1.14	-1.65	0.75	0.17	-2.57
	βh	**-10.86**	**-7.39**	*11.92*	*5.57*	*5.75*	**-11.94**	**-4.88**
	βc	**-8.27**	**-47.21**	*58.88*	**-3.37**	*37.93*	**-56.86**	*8.27*
	βg	*1.07*	**-7.41**	*19.90*	**-12.99**	*8.22*	**-12.61**	*4.90*
		INC-PTM	INC-ALV	PTM-ALV	ALV-M3DL	ALV-M3DB	PTM-M2DL	PTM-M2DB
	DIFFERENCE VECTOR	-0.13	-2.84	-2.77	3.03	4.01	0.70	2.11
	βh	**-1.64**	0.03	**-2.23**	0.24	*1.74*	**-1.67**	*1.63*
	βc	**-11.07**	*2.7*	**-8.75**	0.09	*2.19*	**-2.40**	0.85
	βg	**-14.43**	*15.07*	**-7.51**	-0.22	0.96	-0.16	-0.18
		INC-P3DL	INC-P3DB					
	DIFFERENCE VECTOR	1.85	2.24					
	βh	*1.11*	0.55					
	βc	*1.85*	*2.49*					
	βg	-0.24	0.54					

MANDIBULAR ANALYSIS 1 RAMUS AND CORPUS		MEN-RAM POS	AJUNC-RAM POS	AJUNC-GON	ALVB-GON	RAM POS-GON	MEN-GON	
P. boisei- P. robustus	DIFFERENCE VECTOR	-9.06	7.20	4.53	-4.40	-19.51	1.56	
	β_h	3.54	-0.58	4.32	-0.77	**-4.53**	**-4.81**	
	β_c	**-5.03**	*5.01*	**-2.83**	-0.56	-0.37	*4.79*	
	βg	-0.79	*1.68*	**-1.26**	-0.04	-0.42	0.59	

MANDIBULAR ANALYSIS 2 CORPUS		MEN-ALVB	MEN-IBB	P3D-P4D	P4D-M1D	M1D-M2D	M2D-M3D	ALVB-M2D
P. boisei- P. robustus	DIFFERENCE VECTOR	-0.88	-7.56	0.44	-0.25	2.05	-2.89	-8.58
	β_h	0.36	-0.41	0.02	0.00	-0.51	**-1.96**	-0.21
	β_c	-0.23	**-1.80**	0.24	**-1.15**	0.88	***-5.89***	-0.81
	βg	-0.02	-0.47	0.98	-0.56	-0.35	-0.95	-0.14

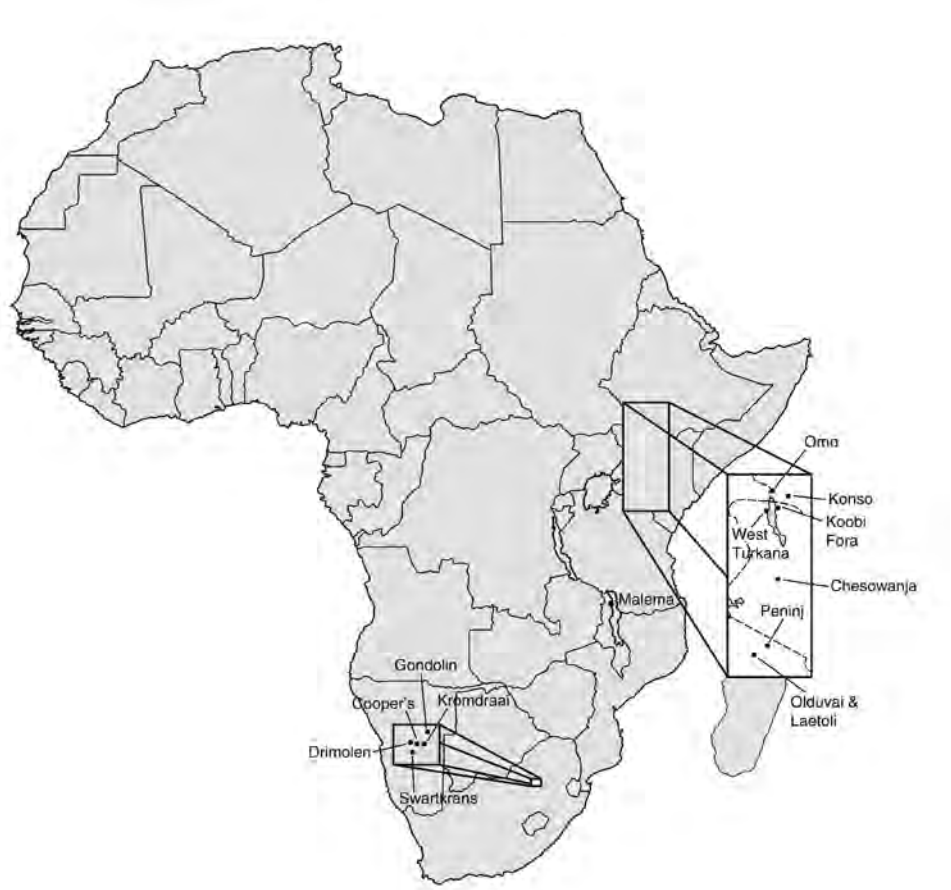

Figure 3.1. Discovery sites of *Paranthropus* showing the distribution of *P. robustus*, *P. boisei* and *P. aethiopicus* across southern and eastern Africa (Wood and Schroer, 2017). Permission for reproduction from B. Wood.

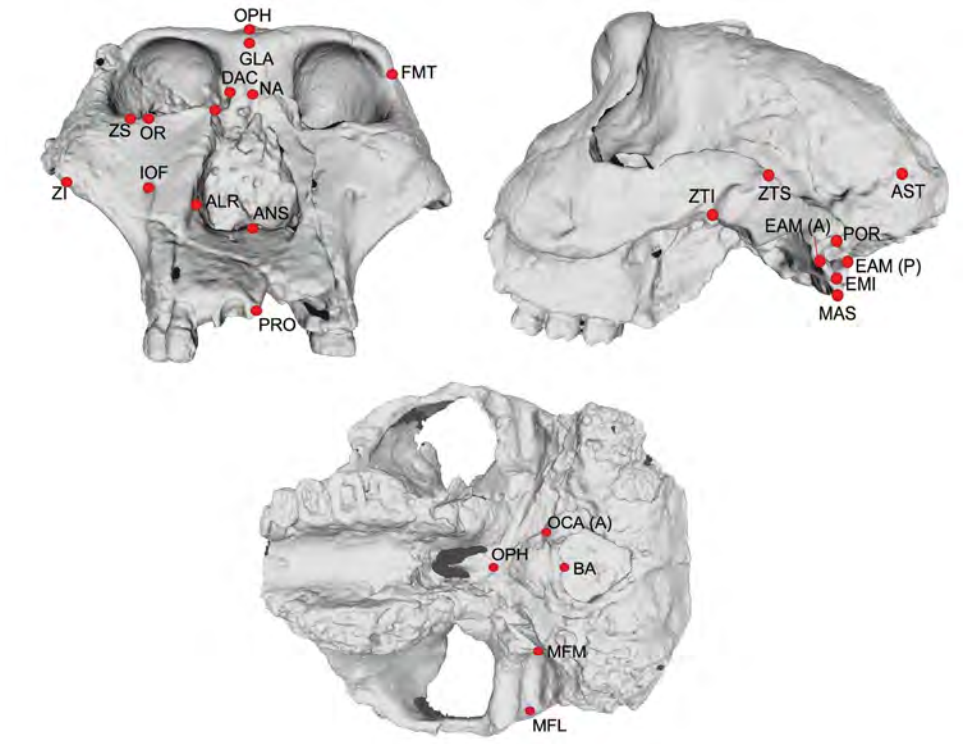

Figure 3.2. Cranial landmark data utilized in this study (frontal and lateral views of SK 48, and inferior view of KNM-ER 406). Landmark abbreviations are described in Table 7.2.

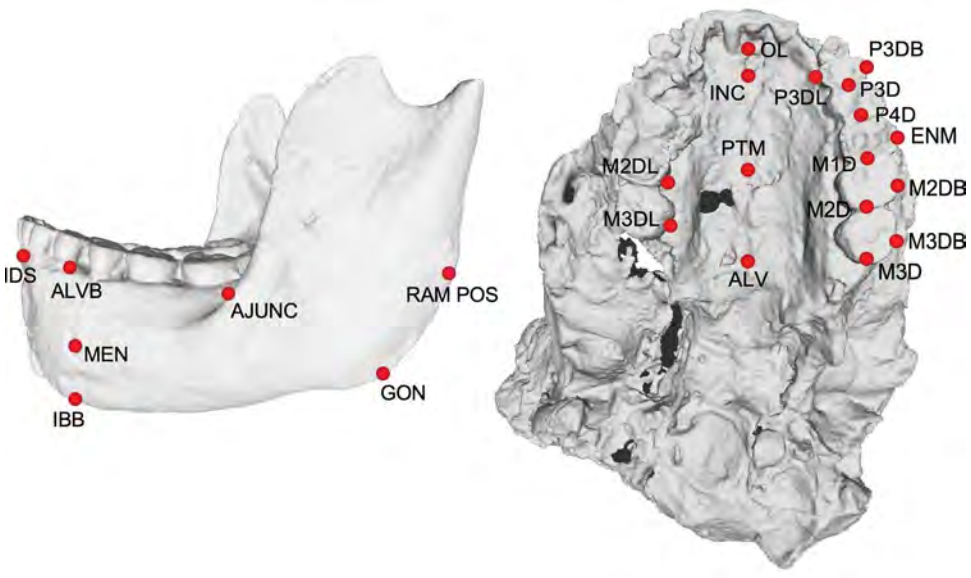

Figure 3.3. Cranial and mandibular landmark data utilized in this study (cranium of SK 83 and mandible of SK 23 depicted). Landmark abbreviations are described in Table 7.2.

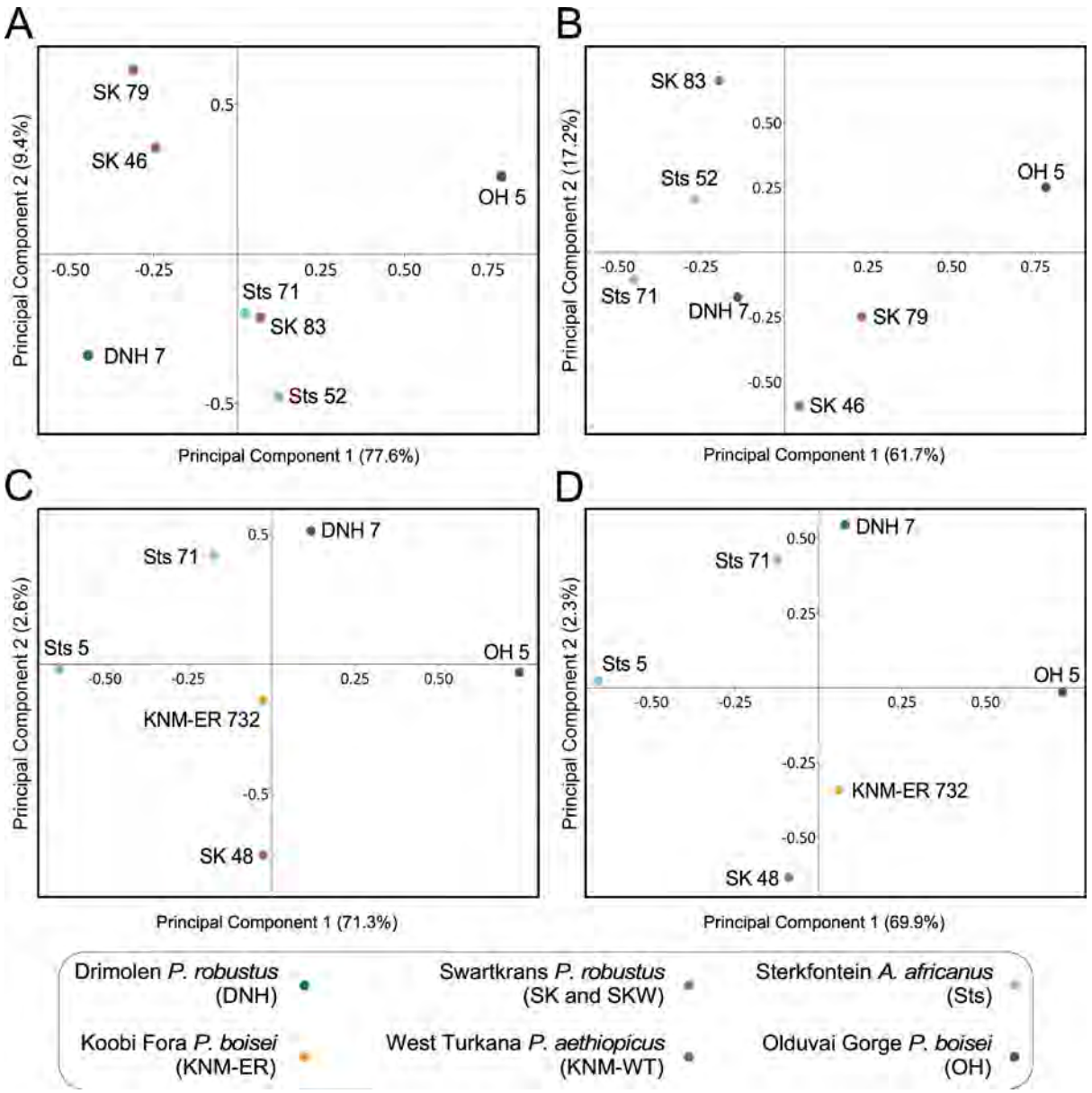
A
SK 79
SK 46
OH 5
Sts 71
SK 83
DNH 7
Sts 52
Principal Component 2 (9.4%)
Principal Component 1 (77.6%)
B
SK 83
Sts 52
OH 5
Sts 71
DNH 7
SK 79
SK 46
Principal Component 2 (17.2%)
Principal Component 1 (61.7%)
C
DNH 7
Sts 71
Sts 5
OH 5
KNM-ER 732
SK 48
Principal Component 2 (2.6%)
Principal Component 1 (71.3%)
D
DNH 7
Sts 71
Sts 5
OH 5
KNM-ER 732
SK 48
Principal Component 2 (2.3%)
Principal Component 1 (69.9%)
Drimolen P. robustus (DNH)
Swartkrans P. robustus (SK and SKW)
Sterkfontein A. africanus (Sts)
Koobi Fora P. boisei (KNM-ER)
West Turkana P. aethiopicus (KNM-WT)
Olduvai Gorge P. boisei (OH)

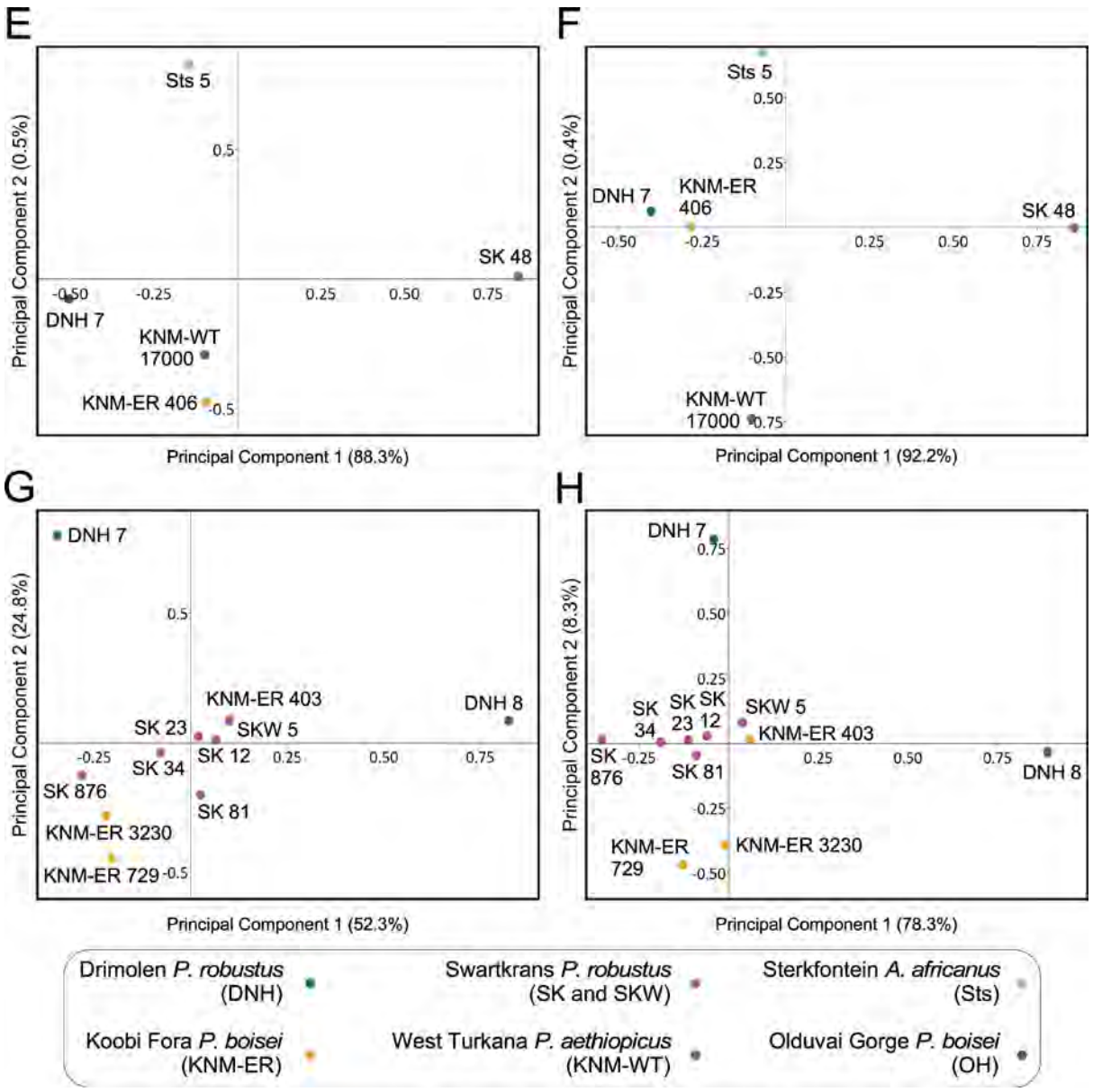

Figure 3.4. A subset of principal coordinates plots of Mahalanobis' distances between fossil specimens, using a *Homo sapiens* and *Gorilla gorilla* variance/covariance model. Percentage of variance explained by each principal coordinate is displayed on each plot. Matrices of Mahalanobis' distances (D^2) can be found in the online dataset. Descriptions of traits used in each analysis are given in Table 7.3. (A) Cranial Analysis 1 (midface/maxilla) with *Homo sapiens* V/CV matrix. (B) Cranial Analysis 1 (midface/maxilla) with *Gorilla gorilla* V/CV

matrix. (C) Cranial Analysis 2 (zygomatic) with *Homo sapiens* V/CV matrix. (D) Cranial Analysis 2 (zygomatic) with *Gorilla gorilla* V/CV matrix. (E) Cranial Analysis 6 (temporal) with *Homo sapiens* V/CV matrix. (F) Cranial Analysis 6 (temporal) with *Gorilla gorilla* V/CV matrix. (G) Mandibular Analysis 2 (ramus and corpus) with *Homo sapiens* V/CV matrix. (H) Mandibular Analysis 2 (corpus) with *Gorilla gorilla* V/CV matrix.

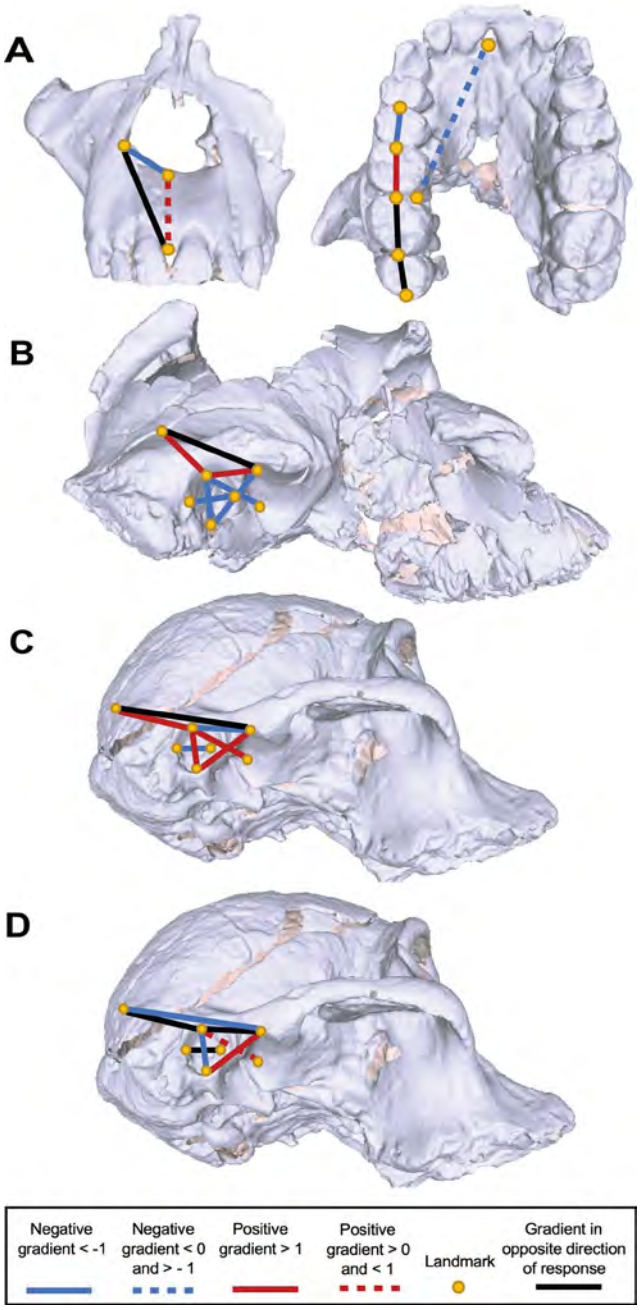

Figure 3.5. Visually represented selection gradients necessary to produce observed differences in cranial morphology. Landmarks are described in Table 7.2. Selection gradient values are presented in Table 7.5. Positive and negative selection gradients are shown in blue and red respectively. Strongly positive (values ≥ 1) and strongly negative (values ≤ -1) selection gradients are represented by solid lines. Weak to moderate selection gradients (0 > values > 1; -1 < values < 0) are displayed as dashed lines. Black lines represent selection gradients that are in the opposite direction of the morphological response. (**A**) Cranial

Analysis 1 (Midface – Maxilla) between *A. africanus* and *P. robustus* using a human V/CV matrix (Sts 52 depicted). (**B**) Cranial Analysis 6 (Temporal) between *P. aethiopicus* and *P. robustus* using a chimpanzee V/CV matrix (KNM-WT 17000 depicted). (**C**) Cranial Analysis 6 (Temporal) between *P. aethiopicus* and *A. africanus* using a chimpanzee V/CV matrix (Sts 5 depicted). (**D**) Cranial Analysis 6 (Temporal) between *P. robustus* and *A. africanus* using a gorilla V/CV matrix (Sts 5 depicted).

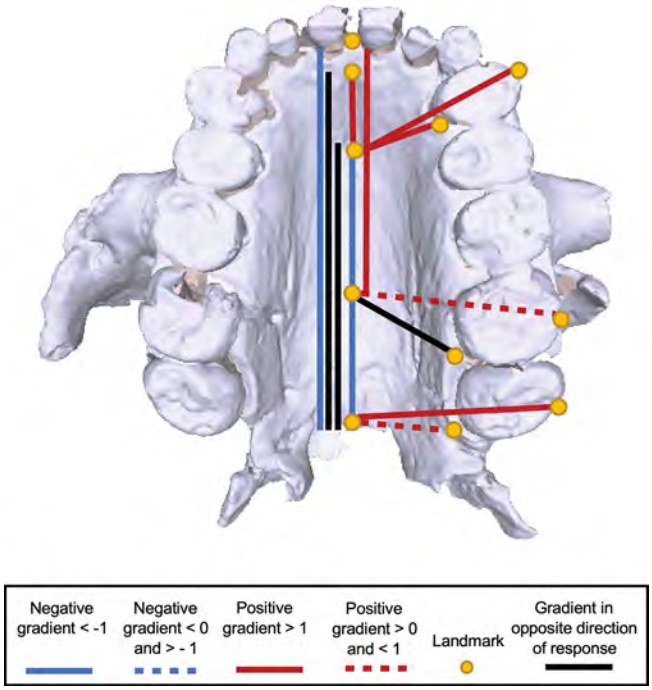

Figure 3.6. Visually represented selection gradients necessary to produce observed differences in palatal morphology (Cranial Analysis 7) between *P. boisei* and *P. robustus* using a chimpanzee V/CV matrix (OH 5 depicted). Landmarks are described in Table 7.2. Selection gradient values are presented in Table 7.5. Positive and negative selection gradients are shown in blue and red respectively. Strongly positive (values ≥ 1) and strongly negative (values ≤ -1) selection gradients are represented by solid lines. Weak to moderate selection gradients (0 > values > 1; -1 < values < 0) are displayed as dashed lines. Black lines represent selection gradients that are in the opposite direction of the morphological response. Selection gradients are placed parallel to one another when there are overlapping traits.

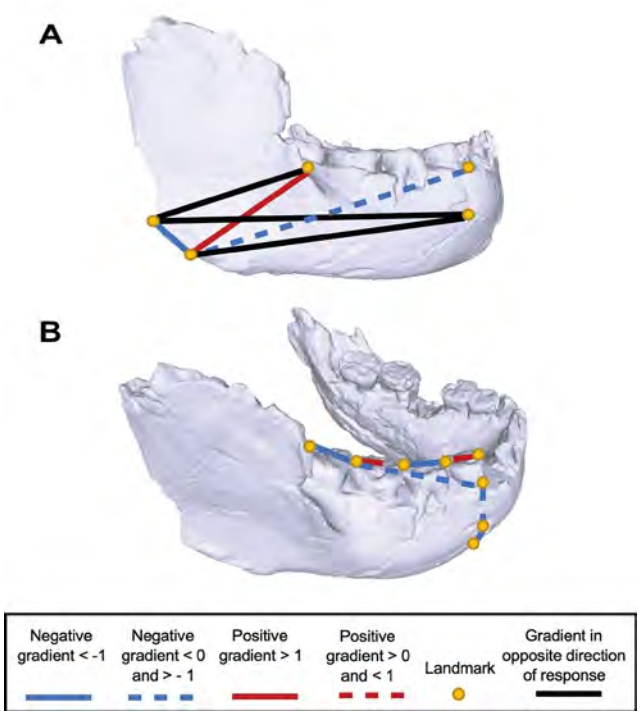

Figure 3.7. Visually represented selection gradients necessary to produce observed differences in mandibular morphology. Landmarks are described in Table 7.2. Selection gradient values are presented in Table 7.5. Positive and negative selection gradients are shown in blue and red respectively. Strongly positive (values ≥ 1) and strongly negative (values ≤ -1) selection gradients are represented by solid lines. Weak to moderate selection gradients (0 > values > 1; -1 < values < 0) are displayed as dashed lines. Black lines represent selection gradients that are in the opposite direction of the morphological response. (**A**) Mandibular Analysis 1 (corpus and ramus) between *P. boisei* and *P. robustus* using a human V/CV matrix (KNM-ER 729 depicted). (**B**) Mandibular Analysis 2 (Corpus) between *P. boisei* and *P. robustus* using a chimpanzee V/CV matrix (KNM-ER 729 depicted).